

# The Effect of Supersymmetric CP Phases on $q\bar{q}$ Annihilations

Aytekin AYDEMIR

*Dept. of Physics, Mersin University, Mersin- Turkey*

Kerem CANKOCAK

*Department of Physics, Mugla University, Mugla- Turkey*

Ramazan SEVER

*Dept. of Physics, Middle East Technical University, Ankara- Turkey*

(November 19, 2018)

## Abstract

We compute the rates for  $q\bar{q}$  annihilation into charginos and neutralinos by taking into account the effects of supersymmetric soft phases. In particular, the phase of the  $\mu$  parameter gains direct accessibility via the production of dissimilar charginos and neutralinos. The phases of the trilinear soft masses do not have a significant effect on the cross sections. Our results can be important for sparticle searches at the LHC.

Keywords :Supersymmetry, MSSM, neutralino and chargino production, Drell-Yan process.

PACS numbers:14.80.Ly, 12.15.Ji, 12.60.Jv

## I. INTRODUCTION

Supersymmetry (SUSY), is one of the most favored extensions of the SM which is capable of stabilizing the ino-sector of fundamental scalars against the ultraviolet divergences. The (soft) breaking of SUSY, around the TeV scale, brings about two new ingredients compared to the standard electroweak theory (SM): First, there are novel sources of flavor violation coming through the off-diagonal entries of the squark mass matrices. Second, there are novel sources of CP violation coming from the phases of the soft masses. The first effect, which cannot be determined theoretically, is strongly constrained by the FCNC data [1], and therefore, as a predictive case, it is convenient to restrict all flavor-violating transitions to the charged-current interactions where they proceed via the known CKM angles. However, this very restriction of the flavor violation to the SM one does not evade new sources of CP violation. Indeed, the model possesses various flavor-blind CP-odd phases contained in the complex  $\mu$  parameter,  $A$  parameters, and gauge fermion masses  $M_i$ .

These phases form the new sources of CP violation which shows up in the electric dipole moments (EDMs) of leptons and hadrons (See [2] and references therein). For heavy quark EDMs see [3]) and for the rate asymmetries of various heavy-light mesons [4]. Therefore, it is of fundamental importance to determine appropriate collider processes where all or some of the SUSY CP phases can be inferred or measured. In fact, the effects of the SUSY CP phases on the Higgs production have been already analyzed in [5,6]. In this work we will discuss the chargino and neutralino production at LHC energies and ways of isolating the phase of the  $\mu$  parameter from the cross section. We shall compute the cross section for  $q\bar{q} \rightarrow \tilde{\chi}_i^+ \tilde{\chi}_j^-$  as a function of  $\varphi_\mu = \text{Arg}[\mu]$  for various values of  $|\mu|$  and the SU(2) gaugino masses  $M_1, M_2$ . We shall also compute the cross section for  $q\bar{q} \rightarrow \tilde{\chi}_i^0 \tilde{\chi}_j^0$  for various SUSY parameters.

## II. $Q\bar{Q} \rightarrow \tilde{\chi}_I^+ \tilde{\chi}_J^-$

Our analysis is similar to that used for the linear collider processes [7]. The relevant Feynman diagrams are depicted in Fig. 1. In what follows we mainly deal with the first two diagrams since the third one is suppressed by presumably heavy squarks. Then it is obvious that the amplitude for the process depends exclusively on the phases in the chargino sector, *i.e.*, the phase of the  $\mu$  parameter.

Here we summarize the masses and couplings of the charginos for completeness (See [10] for details). The charginos which are the mass eigenstates of charged gauginos and Higgsinos are described by a  $2 \times 2$  mass matrix

$$M_C = \begin{pmatrix} M_2 & \sqrt{2}M_W \cos \beta \\ \sqrt{2}M_W \sin \beta & |\mu|e^{i\varphi_\mu} \end{pmatrix} \quad (1)$$

where  $M_2$  is the SU(2) gaugino mass taken to be real throughout the work. The masses of the charginos as well as their mixing matrices follow from the bi-unitary transformation

$$C_R^\dagger M_C C_L = \text{diag}(m_{\chi_1}, m_{\chi_2}) \quad (2)$$

where  $C_L$  and  $C_R$  are  $2 \times 2$  unitary matrices, and  $m_{\chi_1}, m_{\chi_2}$  are the masses of the charginos  $\chi_1, \chi_2$  such that  $m_{\chi_1} < m_{\chi_2}$ . It is convenient to choose the following explicit parametrization for the chargino mixing matrices:

$$C_L = \begin{pmatrix} \cos \theta_L & \sin \theta_L e^{i\varphi_L} \\ -\sin \theta_L e^{-i\varphi_L} & \cos \theta_L \end{pmatrix} \quad (3)$$

$$C_R = \begin{pmatrix} \cos \theta_R & \sin \theta_R e^{i\varphi_R} \\ -\sin \theta_R e^{-i\varphi_R} & \cos \theta_R \end{pmatrix} \cdot \begin{pmatrix} e^{i\phi_1} & 0 \\ 0 & e^{i\phi_2} \end{pmatrix} \quad (4)$$

where the angle parameters  $\theta_{L,R}$ ,  $\varphi_{L,R}$ , and  $\phi_{1,2}$  can be determined from the defining equation (1). A straightforward calculation yields

$$\begin{aligned}
\tan 2\theta_L &= \frac{\sqrt{8}M_W \sqrt{M_2^2 \cos^2 \beta + |\mu|^2 \sin^2 \beta + |\mu|M_2 \sin 2\beta \cos \varphi_\mu}}{M_2^2 - |\mu|^2 - 2M_W^2 \cos 2\beta} \\
\tan 2\theta_R &= \frac{\sqrt{8}M_W \sqrt{|\mu|^2 \cos^2 \beta + M_2^2 \sin^2 \beta + |\mu|M_2 \sin 2\beta \cos \varphi_\mu}}{M_2^2 - |\mu|^2 + 2M_W^2 \cos 2\beta} \\
\tan \varphi_L &= \frac{|\mu| \sin \varphi_\mu}{M_2 \cot \beta + |\mu| \cos \varphi_\mu} \\
\tan \varphi_R &= -\frac{|\mu| \cot \beta \sin \varphi_\mu}{|\mu| \cot \beta \cos \varphi_\mu + M_2}
\end{aligned} \tag{5}$$

in terms of which the remaining two angles  $\phi_1$  and  $\phi_2$  read as follows

$$\tan \phi_i = \frac{\text{Im}[Q_i]}{\text{Re}[Q_i]} \tag{6}$$

where  $i = 1, 2$  and

$$\begin{aligned}
Q_1 &= \sqrt{2}M_W [\cos \beta \sin \theta_L \cos \theta_R e^{-i\varphi_L} + \sin \beta \cos \theta_L \sin \theta_R e^{i\varphi_R}] \\
&\quad + M_2 \cos \theta_L \cos \theta_R + |\mu| \sin \theta_L \sin \theta_R e^{i(\varphi_\mu + \varphi_R - \varphi_L)} \\
Q_2 &= -\sqrt{2}M_W [\cos \beta \sin \theta_R \cos \theta_L e^{-i\varphi_R} + \sin \beta \cos \theta_R \sin \theta_L e^{i\varphi_L}] \\
&\quad + M_2 \sin \theta_L \sin \theta_R e^{i(\varphi_L - \varphi_R)} + |\mu| \cos \theta_L \cos \theta_R e^{i\varphi_\mu}.
\end{aligned} \tag{7}$$

The origin of the phases  $\theta_{L,R}$ ,  $\varphi_{L,R}$ , and  $\phi_{1,2}$  is easy to trace back. The angles  $\theta_L$  and  $\theta_R$  would be sufficient to diagonalize, respectively, the quadratic mass matrices  $M_C^\dagger M_C$  and  $M_C M_C^\dagger$  if  $M_C$  were real. As a result one needs the additional phases  $\varphi_{L,R}$  which are identical to the phases in the off-diagonal entries of the matrices  $M_C^\dagger M_C$  and  $M_C M_C^\dagger$ , respectively. However, these four phases are still not sufficient for making the chargino masses real positive due to the bi-unitary nature of the transformation, and hence, the phases  $\phi_1$  and  $\phi_2$  can not also be made real positive. Finally, inserting the unitary matrices  $C_L$  and  $C_R$  into the defining equation (1) one obtains the following expressions for the masses of the charginos

$$\begin{aligned}
m_{\chi_{1(2)}}^2 &= \frac{1}{2} \left\{ M_2^2 + |\mu|^2 + 2M_W^2 - (+) [(M_2^2 - |\mu|^2)^2 + 4M_W^4 \cos^2 2\beta \right. \\
&\quad \left. + 4M_W^2 (M_2^2 + |\mu|^2 + 2M_2 |\mu| \sin 2\beta \cos \varphi_\mu)]^{1/2} \right\}.
\end{aligned} \tag{8}$$

The fundamental SUSY parameters  $M_2$ ,  $|\mu|$ ,  $\tan\beta$  and the phase parameter  $\cos\varphi_\mu$  can be extracted from the chargino  $\tilde{\chi}_{1,2}^\pm$  parameters [7] *i.e.* the masses  $m_{\tilde{\chi}_{1,2}^\pm}$  and the two mixing angles  $\phi_L$  and  $\phi_R$  of the left and right chiral components of the wave function. These mixing angles are physical observables and they can be measured just like the chargino masses  $m_{\tilde{\chi}_{1,2}^\pm}$  in the process  $q + \bar{q} \rightarrow \tilde{\chi}_i^+ + \tilde{\chi}_j^-$ . The two angles  $\phi_L$  and  $\phi_R$  and the nontrivial phase angles  $\{\varphi_L, \varphi_R, \phi_1, \phi_2\}$  define the couplings of the chargino-chargino-Z vertices:

$$\begin{aligned}
\langle \tilde{\chi}_{1L}^- | Z | \tilde{\chi}_{1L}^- \rangle &= -\frac{e}{s_W c_W} \left[ s_W^2 - \frac{3}{4} - \frac{1}{4} \cos 2\theta_L \right] \\
\langle \tilde{\chi}_{1L}^- | Z | \tilde{\chi}_{2L}^- \rangle &= +\frac{e}{4s_W c_W} e^{-i\varphi_L} \sin 2\theta_L \\
\langle \tilde{\chi}_{2L}^- | Z | \tilde{\chi}_{2L}^- \rangle &= -\frac{e}{s_W c_W} \left[ s_W^2 - \frac{3}{4} + \frac{1}{4} \cos 2\theta_L \right] \\
\langle \tilde{\chi}_{1R}^- | Z | \tilde{\chi}_{1R}^- \rangle &= -\frac{e}{s_W c_W} \left[ s_W^2 - \frac{3}{4} - \frac{1}{4} \cos 2\theta_R \right] \\
\langle \tilde{\chi}_{1R}^- | Z | \tilde{\chi}_{2R}^- \rangle &= +\frac{e}{4s_W c_W} e^{-i(\varphi_R - \phi_1 + \phi_2)} \sin 2\theta_R \\
\langle \tilde{\chi}_{2R}^- | Z | \tilde{\chi}_{2R}^- \rangle &= -\frac{e}{s_W c_W} \left[ s_W^2 - \frac{3}{4} + \frac{1}{4} \cos 2\theta_R \right]
\end{aligned} \tag{9}$$

where  $s_W = \sin\theta_W$  is the weak angle. Note that every vertex here is an explicit function of  $\varphi_\mu$  via the various mixing angles. However, the  $Z$  coupling to unlike charginos  $\tilde{\chi}_i^+ \tilde{\chi}_j^-$  is manifestly complex, and its phase vanishes in the CP-conserving limit,  $\varphi_\mu \rightarrow 0, \pi$ .

Obviously, the photon vertex is independent of the SUSY phases:

$$\langle \tilde{\chi}_{iL,R}^- | \gamma | \tilde{\chi}_{jL,R}^- \rangle = e\delta_{ij} \tag{10}$$

The process  $q\bar{q} \rightarrow \tilde{\chi}_i^+ \tilde{\chi}_j^-$  is generated by the two mechanisms shown in Fig. 1.: the  $s$ -channel  $\gamma$  and  $Z$  exchanges, and  $t$ -channel  $\tilde{q}$  exchange, where the latter is consistently neglected below. The transition amplitude can be parameterized as

$$T(q\bar{q} \rightarrow \tilde{\chi}_i^+ \tilde{\chi}_j^-) = \frac{e^2}{s} Q_{\alpha\beta} [\bar{v}(q) \gamma_\mu P_\alpha u(q)] [\bar{u}(\tilde{\chi}_i^-) \gamma^\mu P_\beta v(\tilde{\chi}_j^+)] \quad (11)$$

where the charges  $Q_{\alpha\beta}$  are defined such that the first index corresponds to the chirality of the  $\bar{q}q$  current and the second one to chargino current. For various final states, their expressions are given by:

(i)  $\tilde{\chi}_1^- \tilde{\chi}_1^+$  for  $q = u, c$

$$Q_{LL} = 1 + \frac{D_Z}{s_W^2 c_W^2} \left( \frac{1}{2} - \frac{2}{3} s_W^2 \right) \left( s_W^2 - \frac{3}{4} - \frac{1}{4} \cos 2\phi_L \right)$$

$$Q_{LR} = 1 + \frac{D_Z}{s_W^2 c_W^2} \left( \frac{1}{2} - \frac{2}{3} s_W^2 \right) \left( s_W^2 - \frac{3}{4} - \frac{1}{4} \cos 2\phi_R \right)$$

$$Q_{RL} = 1 + \frac{D_Z}{c_W^2} \left( -\frac{2}{3} \right) \left( s_W^2 - \frac{3}{4} - \frac{1}{4} \cos 2\phi_L \right)$$

$$Q_{RR} = 1 + \frac{D_Z}{c_W^2} \left( -\frac{2}{3} \right) \left( s_W^2 - \frac{3}{4} - \frac{1}{4} \cos 2\phi_R \right) \quad (12)$$

(ii)  $\tilde{\chi}_1^- \tilde{\chi}_1^+$  for  $q = d, s$

$$Q_{LL} = 1 + \frac{D_Z}{s_W^2 c_W^2} \left( -\frac{1}{2} + \frac{1}{3} s_W^2 \right) \left( s_W^2 - \frac{3}{4} - \frac{1}{4} \cos 2\phi_L \right)$$

$$Q_{LR} = 1 + \frac{D_Z}{s_W^2 c_W^2} \left( -\frac{1}{2} + \frac{1}{3} s_W^2 \right) \left( s_W^2 - \frac{3}{4} - \frac{1}{4} \cos 2\phi_R \right)$$

$$Q_{RL} = 1 + \frac{D_Z}{c_W^2} \left( +\frac{1}{3} \right) \left( s_W^2 - \frac{3}{4} - \frac{1}{4} \cos 2\phi_L \right)$$

$$Q_{RR} = 1 + \frac{D_Z}{c_W^2} \left( +\frac{1}{3} \right) \left( s_W^2 - \frac{3}{4} - \frac{1}{4} \cos 2\phi_R \right) \quad (13)$$

(iii)  $\tilde{\chi}_1^- \tilde{\chi}_2^+$  for  $q = u, c$

$$\begin{aligned}
Q_{LL} &= \frac{D_Z}{4s_W^2 c_W^2} \left( \frac{1}{2} - \frac{2}{3} s_W^2 \right) e^{-i\varphi_L} \sin 2\phi_L \\
Q_{LR} &= \frac{D_Z}{4s_W^2 c_W^2} \left( \frac{1}{2} - \frac{2}{3} s_W^2 \right) e^{-i(\varphi_R - \phi_1 + \phi_2)} \sin 2\phi_R \\
Q_{RL} &= \frac{D_Z}{4c_W^2} \left( -\frac{2}{3} \right) e^{-i\varphi_L} \sin 2\phi_L \\
Q_{RR} &= \frac{D_Z}{4c_W^2} \left( -\frac{2}{3} \right) e^{-i(\varphi_R - \phi_1 + \phi_2)} \sin 2\phi_R
\end{aligned} \tag{14}$$

(iv)  $\underline{\tilde{\chi}_1^- \tilde{\chi}_2^+}$  for  $\underline{q = d, s}$

$$\begin{aligned}
Q_{LL} &= \frac{D_Z}{4s_W^2 c_W^2} \left( -\frac{1}{2} + \frac{1}{3} s_W^2 \right) e^{-i\varphi_L} \sin 2\phi_L \\
Q_{LR} &= \frac{D_Z}{4s_W^2 c_W^2} \left( -\frac{1}{2} + \frac{1}{3} s_W^2 \right) e^{-i(\varphi_R - \phi_1 + \phi_2)} \sin 2\phi_R \\
Q_{RL} &= \frac{D_Z}{4c_W^2} \left( +\frac{1}{3} \right) e^{-i\varphi_L} \sin 2\phi_L \\
Q_{RR} &= \frac{D_Z}{4c_W^2} \left( +\frac{1}{3} \right) e^{-i(\varphi_R - \phi_1 + \phi_2)} \sin 2\phi_R
\end{aligned} \tag{15}$$

(v)  $\underline{\tilde{\chi}_2^- \tilde{\chi}_2^+}$  for  $\underline{q = u, c}$

$$\begin{aligned}
Q_{LL} &= 1 + \frac{D_Z}{s_W^2 c_W^2} \left( \frac{1}{2} - \frac{2}{3} s_W^2 \right) \left( s_W^2 - \frac{3}{4} + \frac{1}{4} \cos 2\phi_L \right) \\
Q_{LR} &= 1 + \frac{D_Z}{s_W^2 c_W^2} \left( \frac{1}{2} - \frac{2}{3} s_W^2 \right) \left( s_W^2 - \frac{3}{4} + \frac{1}{4} \cos 2\phi_R \right) \\
Q_{RL} &= 1 + \frac{D_Z}{c_W^2} \left( -\frac{2}{3} \right) \left( s_W^2 - \frac{3}{4} + \frac{1}{4} \cos 2\phi_L \right) \\
Q_{RR} &= 1 + \frac{D_Z}{c_W^2} \left( -\frac{2}{3} \right) \left( s_W^2 - \frac{3}{4} + \frac{1}{4} \cos 2\phi_R \right)
\end{aligned} \tag{16}$$

(vi)  $\underline{\tilde{\chi}_2^- \tilde{\chi}_2^+}$  for  $q = d, s$

$$\begin{aligned}
Q_{LL} &= 1 + \frac{D_Z}{s_W^2 c_W^2} \left(-\frac{1}{2} + \frac{1}{3} s_W^2\right) \left(s_W^2 - \frac{3}{4} + \frac{1}{4} \cos 2\phi_L\right) \\
Q_{LR} &= 1 + \frac{D_Z}{s_W^2 c_W^2} \left(-\frac{1}{2} + \frac{1}{3} s_W^2\right) \left(s_W^2 - \frac{3}{4} + \frac{1}{4} \cos 2\phi_R\right) \\
Q_{RL} &= 1 + \frac{D_Z}{c_W^2} \left(+\frac{1}{3}\right) \left(s_W^2 - \frac{3}{4} + \frac{1}{4} \cos 2\phi_L\right) \\
Q_{RR} &= 1 + \frac{D_Z}{c_W^2} \left(+\frac{1}{3}\right) \left(s_W^2 - \frac{3}{4} + \frac{1}{4} \cos 2\phi_R\right)
\end{aligned} \tag{17}$$

Here all the amplitudes are built up by the  $\gamma$  and  $Z$  exchanges, and  $D(Z)$  stands for the  $Z$  propagator:  $D_Z = s/(s - m_Z^2 + im_Z \Gamma_Z)$ .

In what follows, for convenience we will introduce four combinations of the charges

$$\begin{aligned}
Q_1 &= \frac{1}{4} [ |Q_{RR}|^2 + |Q_{LL}|^2 + |Q_{RL}|^2 + |Q_{LR}|^2 ] \\
Q_2 &= \frac{1}{2} \text{Re} [ Q_{RR} Q_{RL}^* + Q_{LL} Q_{LR}^* ] \\
Q_3 &= \frac{1}{4} [ |Q_{RR}|^2 + |Q_{LL}|^2 - |Q_{RL}|^2 - |Q_{LR}|^2 ] \\
Q_4 &= \frac{1}{2} \text{Im} [ Q_{RR} Q_{RL}^* + Q_{LL} Q_{LR}^* ]
\end{aligned} \tag{18}$$

so that the differential cross section can be expressed simply as

$$\frac{d\sigma}{d \cos \Theta} (q\bar{q} \rightarrow \tilde{\chi}_i^+ \tilde{\chi}_j^-) = \frac{\pi \alpha^2}{2s} \lambda^{1/2} \{ [1 - (\mu_i^2 - \mu_j^2)^2 + \lambda \cos^2 \Theta] Q_1 + 4\mu_i \mu_j Q_2 + 2\lambda^{1/2} Q_3 \cos \Theta \} \tag{19}$$

with the usual two body phase space factor:

$$\lambda(1, \mu_i^2, \mu_j^2) = [1 - (\mu_i + \mu_j)^2][1 - (\mu_i - \mu_j)^2] \tag{20}$$

defined via the reduced mass  $\mu_i^2 = m_{\tilde{\chi}_i^\pm}^2/s$ .



Integrating the differential cross section over the center-of-mass scattering angle  $\Theta$  we arrive at the total cross section

$$\sigma = \sigma(\varphi_\mu, \mu, M_2, s, \tan \beta) \quad (21)$$

whose dependencies on  $\varphi_\mu$ ,  $M_2$  and  $|\mu|$  will be analyzed numerically.

Besides the total cross section, it is necessary to analyze the rate asymmetries for having better information about  $\varphi_\mu$ . Concerning this point, we investigate the normal polarization vector of the charginos which are inherently CP-odd and exist therefore if CP is broken in the fundamental theory.

Defining the polarization vector  $\vec{P} = (P_L, P_T, P_N)$  in the rest frame of the chargino, where  $P_L$  denotes the component parallel to the charginos flight direction,  $P_T$  the transverse component in the production plane, and  $P_N$  is the component normal to the production plane, these three components can be expressed by helicity amplitudes in the following way [8]:

$$\begin{aligned} P_L &= \frac{1}{4} \sum_{\sigma=\pm} \left\{ |\langle \sigma; ++ \rangle|^2 + |\langle \sigma; +- \rangle|^2 - |\langle \sigma; -+ \rangle|^2 - |\langle \sigma; -- \rangle|^2 \right\} / N \\ P_T &= \frac{1}{2} \text{Re} \left\{ \sum_{\sigma=\pm} [|\langle \sigma; ++ \rangle \langle \sigma; -+ \rangle^* + |\langle \sigma; -- \rangle \langle \sigma; +- \rangle^*] \right\} / N \\ P_N &= \frac{1}{2} \text{Im} \left\{ \sum_{\sigma=\pm} [|\langle \sigma; -- \rangle \langle \sigma; +- \rangle^* - |\langle \sigma; ++ \rangle \langle \sigma; -+ \rangle^*] \right\} / N \end{aligned} \quad (22)$$

The longitudinal and transverse components are P-odd and CP-even. The normal component is P-even and CP-odd, and it can be generated by complex production amplitudes, c.f. Ref. [9].

Therefore, the normal polarization vector is defined as:

$$P_N = 8\lambda^{1/2} \mu_j \sin \Theta \frac{Q_4}{N} \quad (23)$$

for  $\tilde{\chi}_j^+ \tilde{\chi}_j^-$ , the  $j$ -th chargino, and is defined as:

$$\begin{aligned} P_N[\tilde{\chi}_{i,j}^\pm] &= \pm 4\lambda^{1/2} \mu_{j,i} (F_R^2 - F_L^2) \sin \Theta \sin 2\phi_L \\ &\quad \times \sin 2\phi_R \sin(\beta_L - \beta_R + \gamma_1 - \gamma_2) / N \end{aligned} \quad (24)$$

for non-diagonal pairs  $\tilde{\chi}_i^+ \tilde{\chi}_j^-$  where  $i \neq j$ . Here

$$N = 4[(1 - (\mu_i^2 - \mu_j^2)^2 + \lambda \cos^2 \Theta)Q_1 + 4\mu_i\mu_j Q_2 + 2\lambda^{1/2}Q_3 \cos \Theta] \quad (25)$$

and

$$F_R = \frac{D_Z}{4c_W^2}, \quad F_L = \frac{D_Z}{4s_W^2 c_W^2} (s_W^2 - \frac{1}{2}). \quad (26)$$

The polarization can be measured from the two final-state leptons, in the  $\tilde{\chi}_{1,2}^\pm$  leptonic decays. A non-vanishing  $P_N$  will be sufficient to establish non-vanishing CP violation in the system. Therefore, the value of non-vanishing  $P_N$  implies the strength of the CP invariance breaking in SUSY.

### III. $Q\bar{Q} \rightarrow \tilde{\chi}_I^0 \tilde{\chi}_J^0$

We also calculate neutralino pair production to investigate SUSY parameters, since neutralino masses are relatively small to be produced at LHC energies.

The neutral supersymmetric fermionic partners of the B and  $W^3$  gauge bosons,  $\tilde{B}$  and  $\tilde{W}^3$ , can mix with the neutral supersymmetric fermionic partners of the Higgs bosons,  $\tilde{H}_1^0$  and  $\tilde{H}_2^0$  to form the mass eigenstates.

The neutralino mass matrix is

$$M_N = \begin{pmatrix} M_1 e^{i\varphi_1} & 0 & -m_Z s_w c_\beta & m_Z s_w s_\beta \\ 0 & M_2 & m_Z c_w c_\beta & -m_Z c_w s_\beta \\ -m_Z s_w c_\beta & m_Z c_w c_\beta & 0 & |\mu| e^{i\varphi_\mu} \\ m_Z s_w s_\beta & -m_Z c_w s_\beta & |\mu| e^{i\varphi_\mu} & 0 \end{pmatrix} \quad (27)$$

whose diagonalization gives the physical states  $\tilde{\chi}_i^0$ , which are called neutralinos.

Since  $M_N$  is a complex, symmetric matrix, it can be diagonalized by just one unitary matrix  $N$ , such that

$$N^* M_N N^\dagger = \text{diag}(m_{\tilde{\chi}_1^0}, m_{\tilde{\chi}_2^0}, m_{\tilde{\chi}_3^0}, m_{\tilde{\chi}_4^0}). \quad (28)$$

The only Feynman diagram considered here is the last one given in Fig. 1, that is s-channel Z exchange.

The matrix element for the process  $q\bar{q} \rightarrow \tilde{\chi}_i^0 \tilde{\chi}_j^0$  is

$$T(q\bar{q} \rightarrow \tilde{\chi}_i^0 \tilde{\chi}_j^0) = \frac{e^2}{s} Q_{\alpha\beta}^{ij} [\bar{v}(\bar{q}) \gamma_\mu P_\alpha u(q)] \times [\bar{u}(\tilde{\chi}_i^0) \gamma^\mu P_\beta v(\tilde{\chi}_j^0)] \quad (29)$$

where the associated quark and neutralino currents are

(i)  $\underline{\tilde{\chi}_1^0 \tilde{\chi}_1^0}$  for  $\underline{q = u, c}$

$$Q_{LL} = + \frac{D_Z}{s_W^2 c_W^2} \left( \frac{1}{2} - \frac{2}{3} s_W^2 \right) Z_{11}$$

$$Q_{LR} = + \frac{D_Z}{s_W^2 c_W^2} \left( \frac{1}{2} - \frac{2}{3} s_W^2 \right) Z_{11}^*$$

$$Q_{RL} = + \frac{D_Z}{c_W^2} \left( -\frac{2}{3} \right) Z_{11}$$

$$Q_{RR} = + \frac{D_Z}{c_W^2} \left( -\frac{2}{3} \right) Z_{11}^* \quad (30)$$

(ii)  $\underline{\tilde{\chi}_1^0 \tilde{\chi}_1^0}$  for  $\underline{q = d, s}$

$$Q_{LL} = + \frac{D_Z}{s_W^2 c_W^2} \left( -\frac{1}{2} + \frac{1}{3} s_W^2 \right) Z_{11}$$

$$Q_{LR} = + \frac{D_Z}{s_W^2 c_W^2} \left( -\frac{1}{2} + \frac{1}{3} s_W^2 \right) Z_{11}^*$$

$$Q_{RL} = + \frac{D_Z}{c_W^2} \left( +\frac{1}{3} \right) Z_{11}$$

$$Q_{RR} = + \frac{D_Z}{c_W^2} \left( +\frac{1}{3} \right) Z_{11}^* \quad (31)$$

and

$$Z_{ij} = \frac{1}{2}(N_{i3}N_{j3}^* - N_{i4}N_{j4}^*) \quad (32)$$

$$Z_{ij}^* = Z_{ij}$$

Using the predefined charge combinations, differential cross section can be expressed as

$$\frac{d\sigma}{d\cos\Theta}(q\bar{q} \rightarrow \tilde{\chi}_1^0\tilde{\chi}_1^0) = \frac{\pi\alpha^2}{2s}\lambda^{1/2}\{[1 + \lambda\cos^2\Theta]Q_1 + 4\mu_1^2Q_2 + 2\lambda^{1/2}Q_3\cos\Theta\} \quad (33)$$

where

$$\lambda(1, \mu_1^2, \mu_1^2) = [1 - 4\mu_1^2] \quad (34)$$

is defined via the reduced mass  $\mu_1^2 = m_{\tilde{\chi}_1^0}^2/s$ .  $Q_1$ ,  $Q_2$ , and  $Q_3$  are as defined before.

Integrating the differential cross section over the center-of-mass scattering angle  $\Theta$  we arrive at the total cross section

$$\sigma = \sigma(M_1, \mu, M_2, s, \tan\beta) \quad (35)$$

whose dependence on  $M_1$ ,  $|\mu|$  and  $s$  will be analyzed numerically for  $M_2 = 150$  GeV and  $\tan\beta = 30$ .

## IV. NUMERICAL ESTIMATES

### A. Chargino production

In this section we will discuss the dependence of the chargino production cross section on  $\varphi_\mu$ ,  $M_2$ ,  $|\mu|$  and  $\sqrt{s}$ . We everywhere apply the existing collider constraint that  $m_{\chi_2} > 104$  GeV.

In Table 1. we give the cross section values for  $q\bar{q} \rightarrow \tilde{\chi}_1^+ \tilde{\chi}_1^-$  and  $q\bar{q} \rightarrow \tilde{\chi}_1^+ \tilde{\chi}_2^-$  where  $M_2 = 150, 200, 250$  GeV,  $\mu = 150, 200, 250$  GeV,  $\tan\beta = 4, 10, 30, 50$ , and  $\varphi_\mu = \pi/3$  are used in the calculations.

In Fig. 2 and Fig. 5 we show the dependence of the cross sections  $q\bar{q} \rightarrow \tilde{\chi}_1^+ \tilde{\chi}_1^-$  and  $q\bar{q} \rightarrow \tilde{\chi}_1^+ \tilde{\chi}_2^-$  on  $\varphi_\mu$  for  $M_2 = 150, 300$  GeV,  $\mu = 150, 300$  GeV, and  $\tan\beta = 30$ .

For the process  $q\bar{q} \rightarrow \tilde{\chi}_1^+ \tilde{\chi}_1^-$ , the dependence of the cross section on  $\varphi_\mu$  is very weak for the light charginos. As seen from the Figs. 3 and 4, the more spectacular enhancement implies the heavier chargino mass.

In Fig. 6 we show the dependence of the cross sections  $q\bar{q} \rightarrow \tilde{\chi}_1^+ \tilde{\chi}_2^-$  on  $\varphi_\mu$  for  $\mu = 150$  GeV, and  $\tan\beta = 30$ , as a function of  $M_2$ . Again, there is small dependence of the cross section on  $\varphi_\mu$ .

The increase of the cross section is tied up to the variation of the chargino masses with the phases. It is clear that as  $\varphi_\mu : 0 \rightarrow \pi$  the mass splitting of the charginos decrease, as expected from the Equation 8. This is an important effect which implies that the cross section is larger than what one would expect from the CP-conserving theory [7].

Apart from the cross section itself, one can analyze various spin and charge asymmetries which are expected to have an enhanced dependence on  $\varphi_\mu$ . The normal polarization in  $q\bar{q} \rightarrow \tilde{\chi}_1^+ \tilde{\chi}_1^-$  is zero since the  $\tilde{\chi}_1^+ \tilde{\chi}_1^- \gamma$  and  $\tilde{\chi}_1^+ \tilde{\chi}_1^- Z$  vertices are real even for non-zero phases in the chargino mass matrix.

In Fig. 7 we show the normal polarization  $P_N$  of the unlike charginos in  $q\bar{q} \rightarrow \tilde{\chi}_1^+ \tilde{\chi}_2^-$  which has a different dependence on the phases. Here again  $M_2 = 150, 300$  GeV,  $\mu = 150, 300$  GeV,  $\tan\beta = 30$ , and  $\varphi_\mu = \pi/2$ .

The dependence of the normal polarization on the value of  $\Theta$  and  $\varphi_\mu$  is shown in Fig. 8, where the normal polarization has its maximum at  $\Theta = \pi/2$  as expected from the Eqn. 23, and at  $\varphi_\mu = \pi/2$  as stated above.

However, we believe that for clarifying the essence of measuring  $\varphi_\mu$  the first quantity to be

tested is the cross section itself.

### B. Neutralino production

In this section, the dependence of the neutralino production cross-section on center of mass energy  $\sqrt{s}$  is investigated for  $\mu = 150, 200$  GeV,  $M_1 = 150, 200$  GeV and for  $M_2 = 150, 200$  GeV. In Fig. 9 we show the dependence of the cross section for  $q\bar{q} \rightarrow \tilde{\chi}_1^0 \tilde{\chi}_1^0$  on  $\sqrt{s}$ , for  $\varphi_\mu = 0, \frac{\pi}{2}, \pi$  and  $\frac{3\pi}{2}$ , where  $M_1 = 150$  GeV,  $M_2 = 100$  GeV and  $\mu = 200$  GeV. The cross-section is maximum at about  $\sqrt{s} = 230$  GeV and drops as  $\sqrt{s}$  becomes higher. The variation of the cross section on  $\varphi_\mu$  is seen clearly. The highest cross section is obtained for  $\varphi_\mu = \pi$ , when  $M_1 < \mu$ , as expected from the CP-conserving theory [7].

In Fig. 10, we show the dependence of the cross section for  $q\bar{q} \rightarrow \tilde{\chi}_1^0 \tilde{\chi}_1^0$  on  $\sqrt{s}$  and  $\mu$ , for  $\varphi_\mu = \frac{\pi}{2}$ ,  $M_1 = 150$  GeV,  $M_2 = 150$  GeV and  $\tan\beta = 30$ .

Finally, in Fig. 11, we plot the cross section for  $q\bar{q} \rightarrow \tilde{\chi}_1^0 \tilde{\chi}_1^0$  as a function of  $\mu$  and  $\varphi_\mu$ , for  $M_1 = 150$  GeV,  $M_2 = 150$  GeV and  $\tan\beta = 30$ . The dependence of the cross section on  $\varphi_\mu$  is seen clearly in this figure. At  $\varphi_\mu = \pi$  the cross section is lowest when  $M_1 > \mu$  and highest when  $M_1 < \mu$  respectively.

## V. DISCUSSION AND CONCLUSION

We have analyzed the production of charginos and neutralinos at LHC energies with the aim of isolating the phase of the  $\mu$  parameter. The measurement of these processes will be an important step for determining the CP violation sources of low-energy supersymmetry. Our numerical results suggest that there is a strong dependence on the phase of the  $\mu$  parameter especially when  $|\mu|$  is comparable to the gaugino masses.

In true experimental environment, the cross sections we have discussed above form the subprocess cross sections to be integrated over appropriate structure functions. However,

given the energy span of LHC that it will be possible to probe sparticles up to 2 TeV, it is clear that the center-of-mass energies we discuss are always within experimental reach. If the experiment concludes  $\varphi_\mu \sim \mathcal{O}(1)$  then, given strong bounds from the absence of permanent EDMs for electron, neutron, atoms and molecules, one would conclude that the first two generations of sfermions will be hierarchically split from the ones in the third generation. In case the experiment reports a small  $\varphi_\mu$  then presumably all sfermion generations can lie right at the weak scale in agreement with the EDM bounds. In this case, where  $\varphi_\mu$  is a small fraction of  $\pi$ , one might expect that the minimal model is UV-completed above the TeV scale such that the  $\mu$  parameter is promoted to a dynamical SM-singlet field (*e.g.* the  $Z'$  models).

## FIGURE CAPTIONS

FIGURE 1. The lowest order Feynman diagrams for  $q\bar{q} \rightarrow \tilde{\chi}_i^+ \tilde{\chi}_j^-$  and  $q\bar{q} \rightarrow \tilde{\chi}_i^0 \tilde{\chi}_j^0$  processes.

FIGURE 2. The plot of cross section for  $q\bar{q} \rightarrow \tilde{\chi}_1^+ \tilde{\chi}_1^-$  as a function of  $\varphi_\mu$  for the values of  $\mu = 150, 300$  GeV,  $M_2 = 150, 300$  GeV and  $\tan\beta = 30$ .

FIGURE 3. The plot of cross section for  $q\bar{q} \rightarrow \tilde{\chi}_1^+ \tilde{\chi}_1^-$  as a function of  $\varphi_\mu$  and  $M_2$ , for the values of  $\mu = 150$  GeV and  $\tan\beta = 30$ .

FIGURE 4. The plot of cross section for  $q\bar{q} \rightarrow \tilde{\chi}_1^+ \tilde{\chi}_1^-$  as a function of  $\varphi_\mu$  and  $\mu$ , for the values of  $M_2 = 200$  GeV and  $\tan\beta = 30$ .

FIGURE 5. The plot of cross section for  $q\bar{q} \rightarrow \tilde{\chi}_1^+ \tilde{\chi}_2^-$  as a function of  $\varphi_\mu$  for the values of  $\mu = 150, 300$  GeV,  $M_2 = 150, 300$  GeV and  $\tan\beta = 30$ .

FIGURE 6. The plot of cross section for  $q\bar{q} \rightarrow \tilde{\chi}_1^+ \tilde{\chi}_2^-$  as a function of  $\varphi_\mu$  and  $M_2$ , for the values of  $\mu = 150$  GeV and  $\tan\beta = 30$ .

FIGURES 7. The plot of normal polarization for  $q\bar{q} \rightarrow \tilde{\chi}_1^+ \tilde{\chi}_2^-$  as a function of  $\Theta$  for the values of  $\mu = 150, 300$  GeV,  $M_2 = 150, 300$  GeV and  $\tan\beta = 30$ , when  $\varphi_\mu = \pi/2$ .

FIGURES 8. 3-dimensional plot of normal polarization for  $q\bar{q} \rightarrow \tilde{\chi}_1^+ \tilde{\chi}_2^-$  as a function of  $\Theta$  and  $\varphi_\mu$  for the values of  $\mu = 150$  GeV,  $M_2 = 150$  GeV and  $\tan\beta = 30$ .

FIGURE 9. The plot of cross section for  $q\bar{q} \rightarrow \tilde{\chi}_1^0 \tilde{\chi}_1^0$  as a function of  $\sqrt{s}$  for the values of  $\varphi_\mu = 0, \frac{\pi}{2}, \pi$  and  $\frac{3\pi}{2}$ , where  $M_1 = 150$  GeV,  $M_2 = 150$  GeV,  $\mu = 200$  GeV and  $\tan\beta = 30$ .

FIGURE 10. The plot of cross section for  $q\bar{q} \rightarrow \tilde{\chi}_1^0 \tilde{\chi}_1^0$  as a function of  $\sqrt{s}$  and  $\mu$ , where  $\varphi_\mu = \frac{\pi}{2}$ ,  $M_1 = 150$  GeV,  $M_2 = 150$  GeV and  $\tan\beta = 30$ .

FIGURE 11. The plot of cross section for  $q\bar{q} \rightarrow \tilde{\chi}_1^0 \tilde{\chi}_1^0$  as a function of  $\varphi_\mu$  and  $\mu$ , where  $\sqrt{s} = 500$  GeV,  $M_1 = 150$  GeV,  $M_2 = 150$  GeV and  $\tan\beta = 30$ .



## REFERENCES

- [1] F. Gabbiani, E. Gabrielli, A. Masiero and L. Silvestrini, Nucl. Phys. B **477**, 321 (1996) [arXiv:hep-ph/9604387].
- [2] V. D. Barger, T. Falk, T. Han, J. Jiang, T. Li and T. Plehn, Phys. Rev. D **64**, 056007 (2001) [arXiv:hep-ph/0101106].
- [3] D. A. Demir and M. B. Voloshin, Phys. Rev. D **63**, 115011 (2001) [arXiv:hep-ph/0012123].
- [4] D. A. Demir, A. Masiero and O. Vives, Phys. Rev. D **61**, 075009 (2000) [arXiv:hep-ph/9909325]; Phys. Rev. Lett. **82**, 2447 (1999) [arXiv:hep-ph/9812337]; S. w. Baek, J. H. Jang, P. Ko and J. H. Park, Phys. Rev. D **62**, 117701 (2000) [arXiv:hep-ph/9907572]; S. w. Baek and P. Ko, Phys. Rev. Lett. **83**, 488 (1999) [arXiv:hep-ph/9812229]; D. A. Demir and K. A. Olive, Phys. Rev. D **65**, 034007 (2002) [arXiv:hep-ph/0107329]; M. Boz and N. K. Pak, Phys. Lett. B **531**, 119 (2002) [arXiv:hep-ph/0201199].
- [5] D. A. Demir, Phys. Rev. D **60**, 055006 (1999) [arXiv:hep-ph/9901389]; A. Pilaftsis and C. E. Wagner, Nucl. Phys. B **553**, 3 (1999) [arXiv:hep-ph/9902371]; T. Ibrahim and P. Nath, Phys. Rev. D **63**, 035009 (2001) [arXiv:hep-ph/0008237].
- [6] D. A. Demir, Phys. Lett. B **465**, 177 (1999) [arXiv:hep-ph/9809360]; G. L. Kane and L. T. Wang, Phys. Lett. B **488**, 383 (2000) [arXiv:hep-ph/0003198].
- [7] V. D. Barger, T. Han, T. J. Li and T. Plehn, Phys. Lett. B **475**, 342 (2000) [arXiv:hep-ph/9907425]; S. Y. Choi, J. Kalinowski, G. Moortgat-Pick and P. M. Zerwas, Eur. Phys. J. C **22**, 563 (2001) [Addendum-ibid. C **23**, 769 (2002)] [arXiv:hep-ph/0108117]; S. Y. Choi, A. Djouadi, M. Guchait, J. Kalinowski, H. S. Song and P. M. Zerwas, Eur. Phys. J. C **14**, 535 (2000) [arXiv:hep-ph/0002033]; Phys. Lett. B **479**, 235 (2000) [arXiv:hep-ph/0001175]; S. Y. Choi, A. Djouadi, H. K. Dreiner, J. Kalinowski and

- P. M. Zerwas, Eur. Phys. J. C **7**, 123 (1999) [arXiv:hep-ph/9806279].
- [8] S. Y. Choi, A. Djouadi, H. S. Song and P. M. Zerwas, Eur. Phys. J. C **8**, 669 (1999) [arXiv:hep-ph/9812236]
- [9] J.H. Kühn, A. Reiter and P.M. Zerwas, Nucl. Phys. **B272** (1986) 560.
- [10] L. Kneur and G. Moultaka, Phys. Rev. D **61**, 095003 (2000) [arXiv:hep-ph/9907360];  
D. A. Demir, Phys. Rev. D **60**, 095007 (1999) [arXiv:hep-ph/9905571]; P. Nath, Phys. Rev. Lett. **66**, 2565 (1991).

TABLES

TABLE I. The cross section values for  $q\bar{q} \rightarrow \tilde{\chi}_1^+ \tilde{\chi}_1^-$  and  $q\bar{q} \rightarrow \tilde{\chi}_1^+ \tilde{\chi}_2^-$  processes for  $\varphi_\mu = \pi/3$ ,  $\mu = 150, 200, 250$  GeV,  $M_2 = 150, 200, 250$  GeV, and  $\tan\beta = 4, 10, 30, 50$ .

$\tan\beta$	$M_2(\text{GeV})$	$\mu(\text{GeV})$	$\sigma(q\bar{q} \rightarrow \tilde{\chi}_1^+ \tilde{\chi}_1^-)(\text{pb})$	$\sigma(q\bar{q} \rightarrow \tilde{\chi}_1^+ \tilde{\chi}_2^-)(\text{pb})$
4	150	150	4.76	0.25
4	150	200	5.41	0.26
4	150	250	5.90	0.16
4	200	150	4.02	0.15
4	200	200	4.45	0.16
4	200	250	4.93	0.00
4	250	150	3.57	0.07
4	250	200	3.64	0.00
4	250	250	3.75	0.00
10	150	150	4.76	0.24
10	150	200	5.42	0.25
10	150	250	5.91	0.15
10	200	150	3.98	0.14
10	200	200	4.42	0.15
10	200	250	4.91	0.00
10	250	150	3.53	0.06
10	250	200	3.58	0.00
10	250	250	3.66	0.00

continued

30	150	150	4.75	0.24
30	150	200	5.43	0.25
30	150	250	5.92	0.15
30	200	150	3.96	0.14
30	200	200	4.40	0.15
30	200	250	4.89	0.00
30	250	150	3.50	0.06
30	250	200	3.54	0.00
30	250	250	3.60	0.00
50	150	150	4.75	0.24
50	150	200	5.43	0.25
50	150	250	5.92	0.15
50	200	150	3.95	0.14
50	200	200	4.39	0.15
50	200	250	4.89	0.00
50	250	150	3.50	0.06
50	250	200	3.53	0.00
50	250	250	3.59	0.00

FIGURES

FIG. 1.

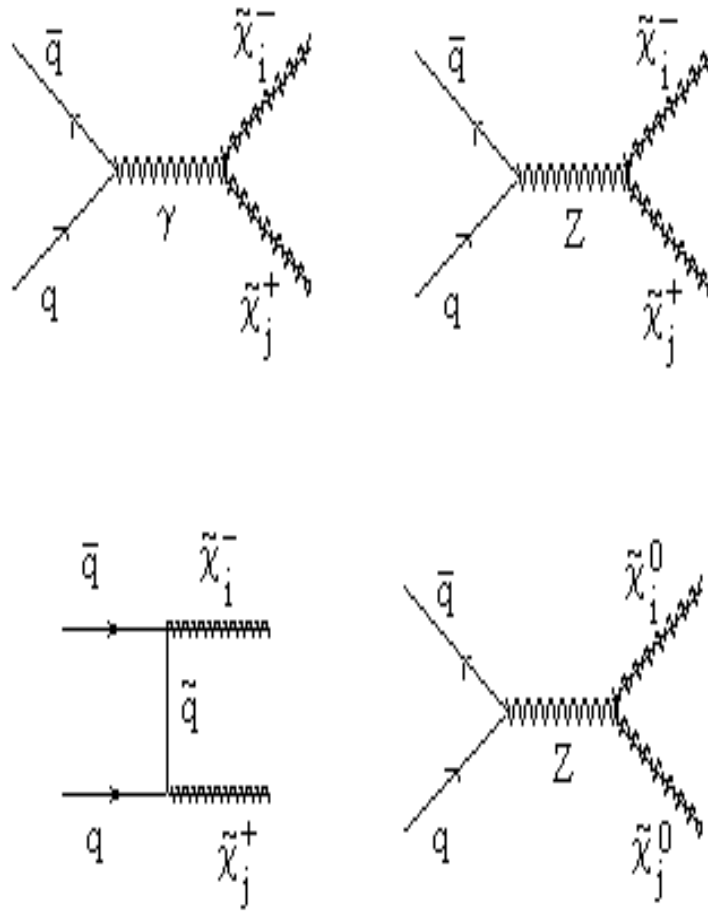


FIG. 2.

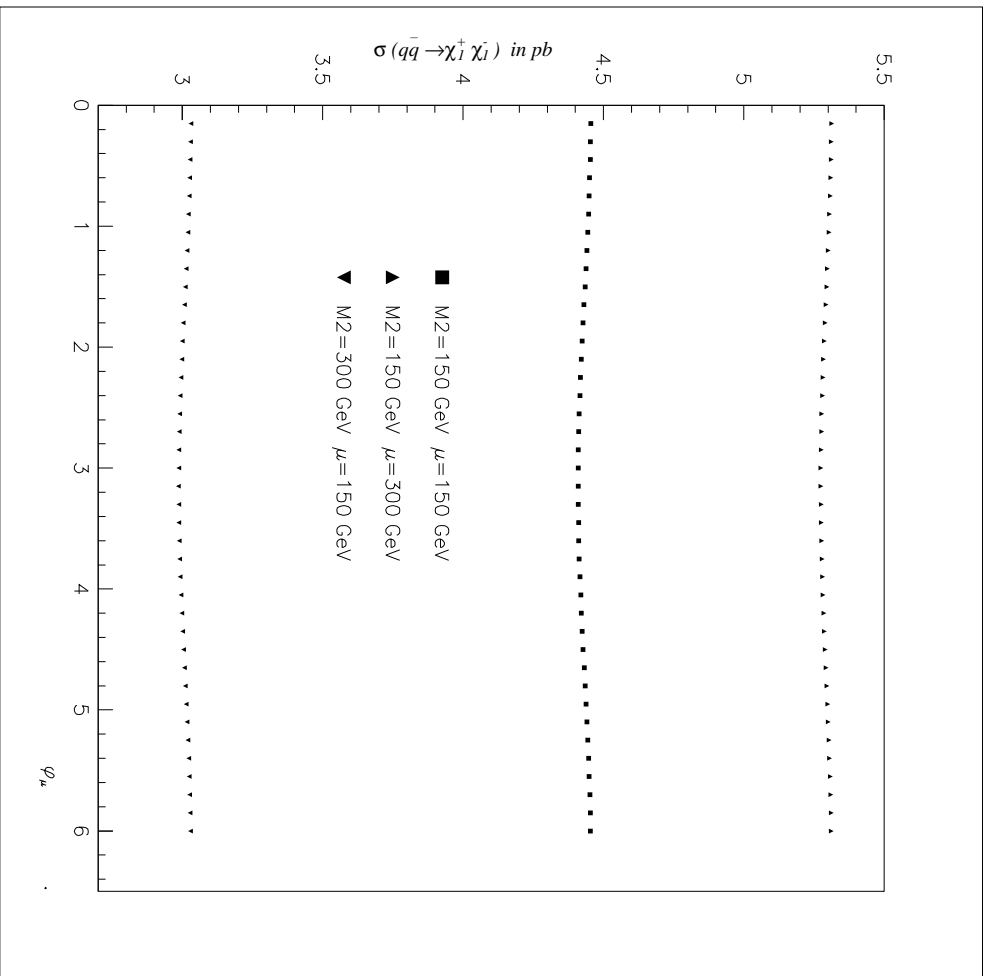


FIG. 3.

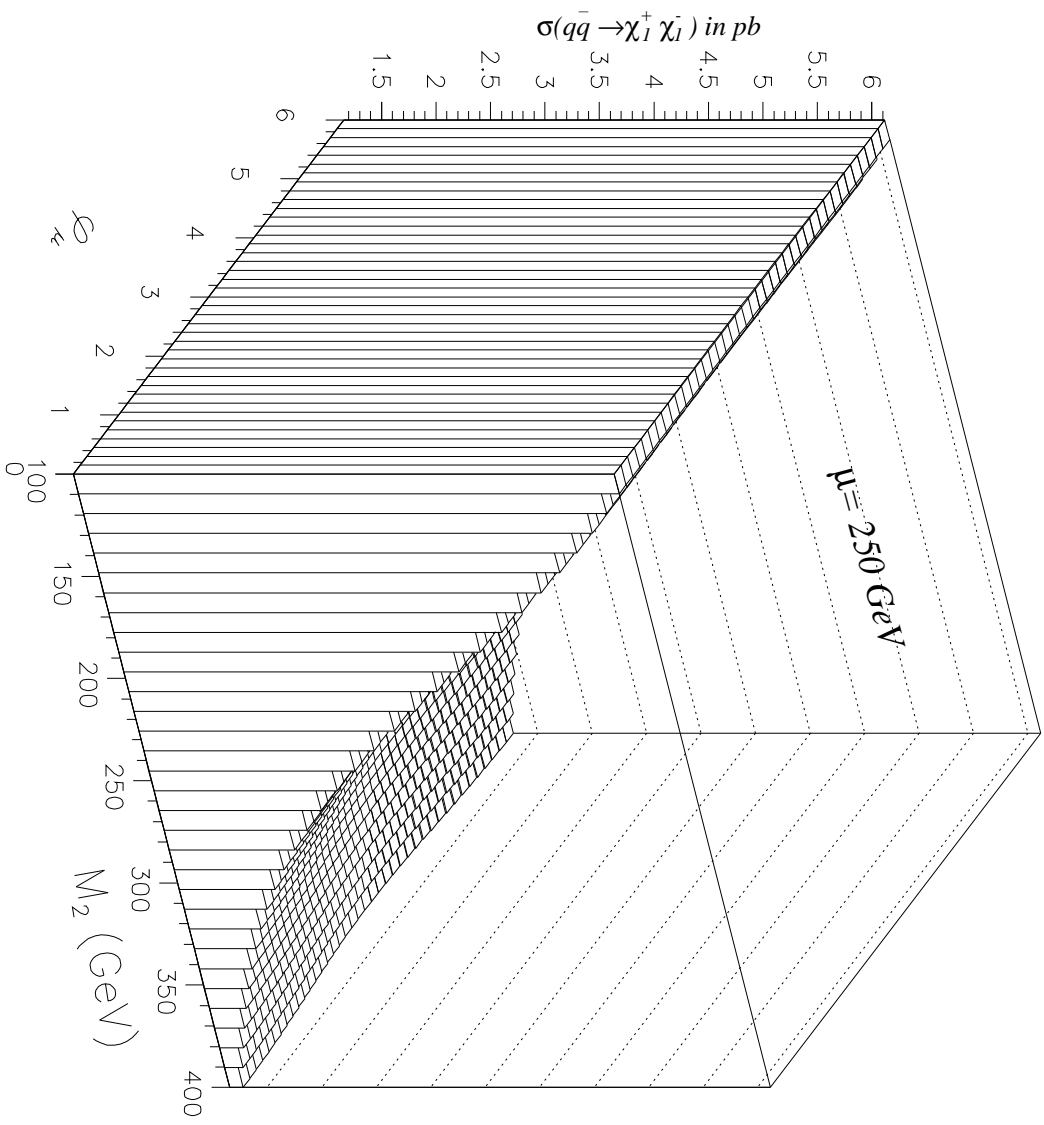


FIG. 4.

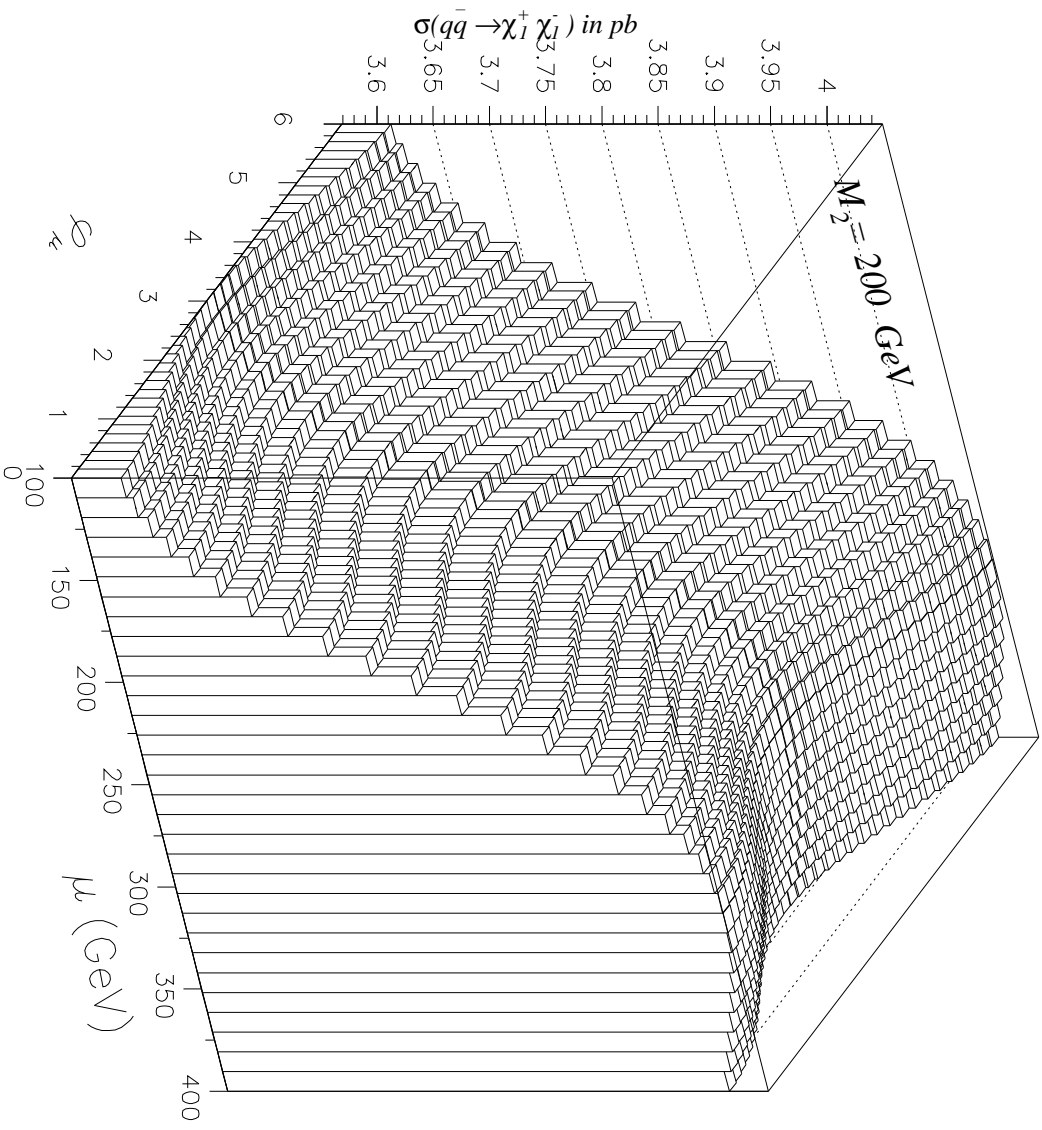




FIG. 5.

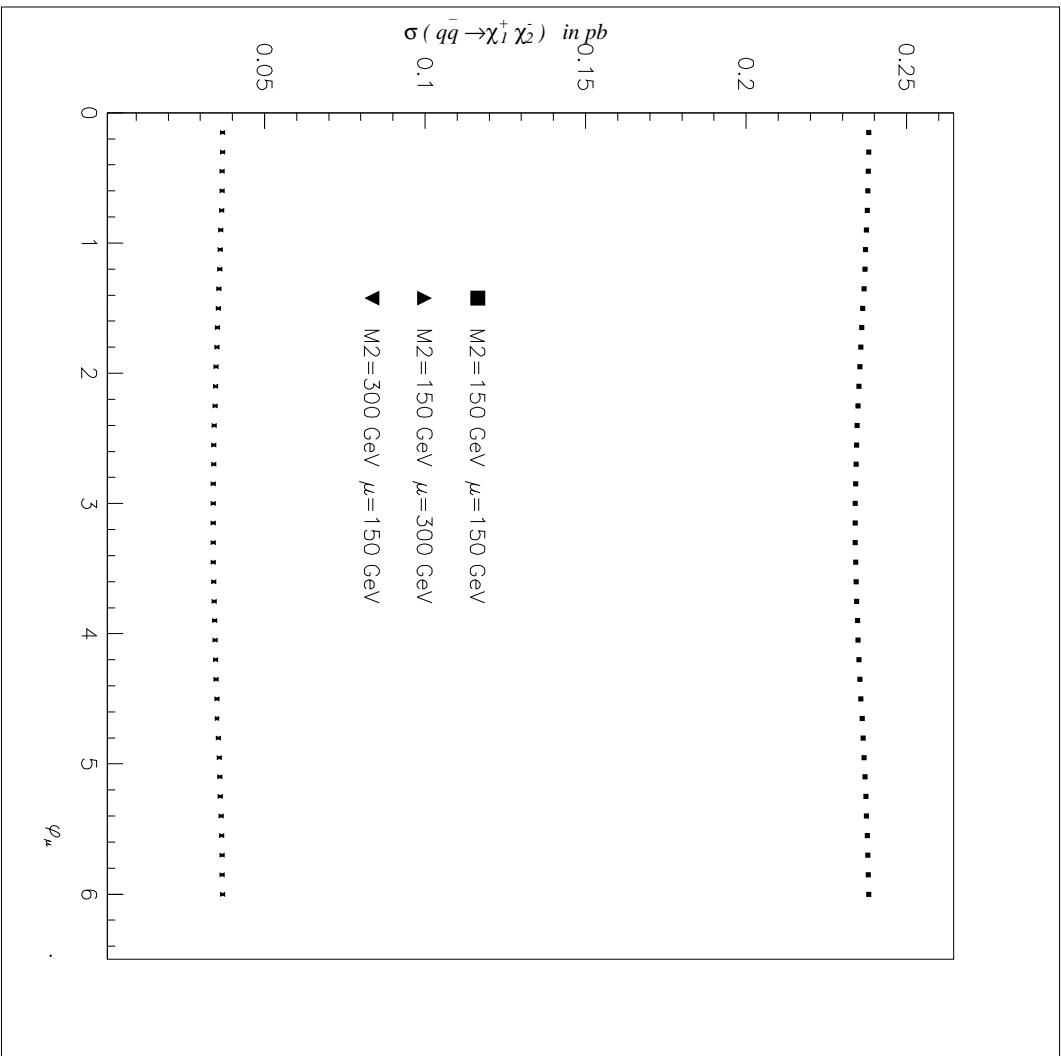


FIG. 6.

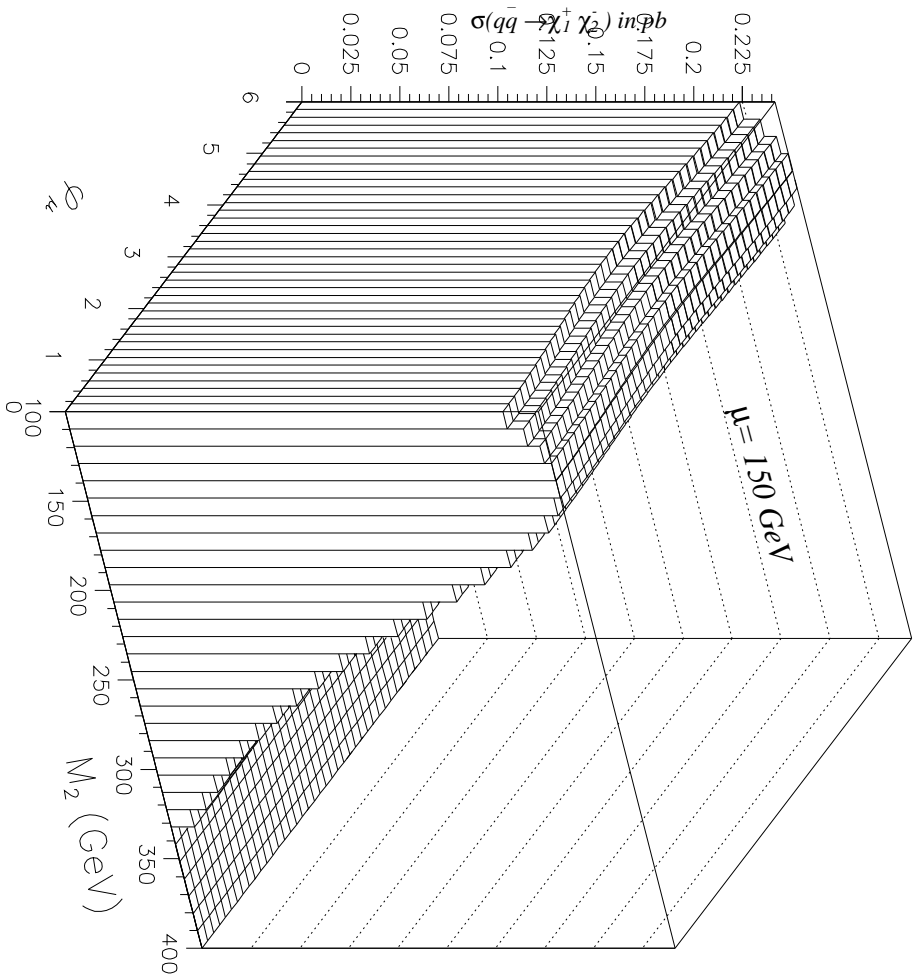


FIG. 7.

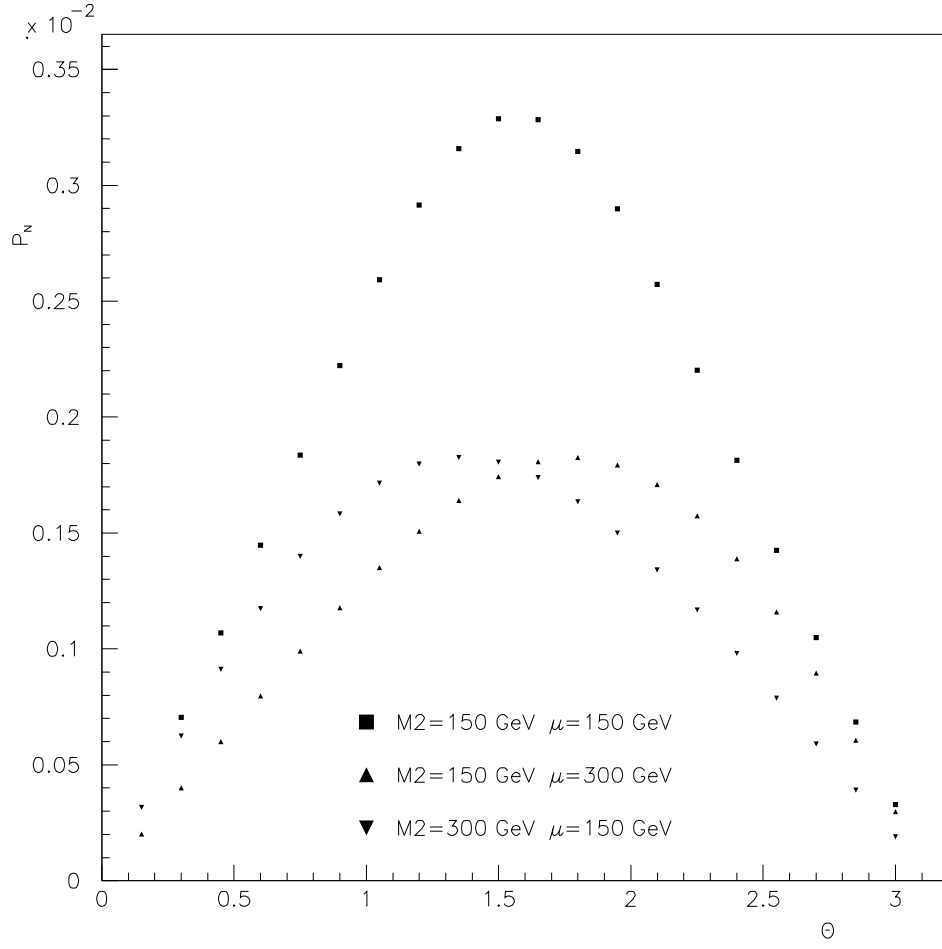


FIG. 8.

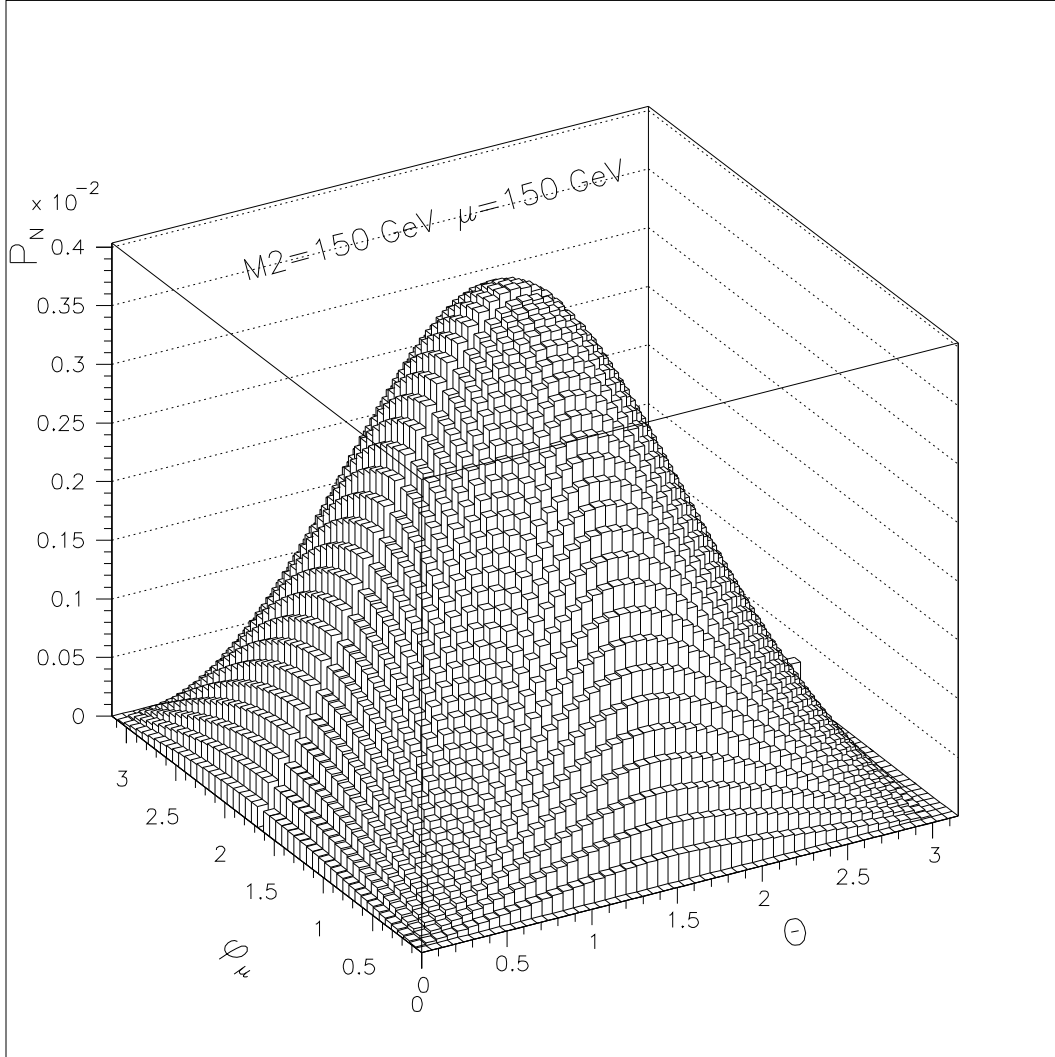


FIG. 9.

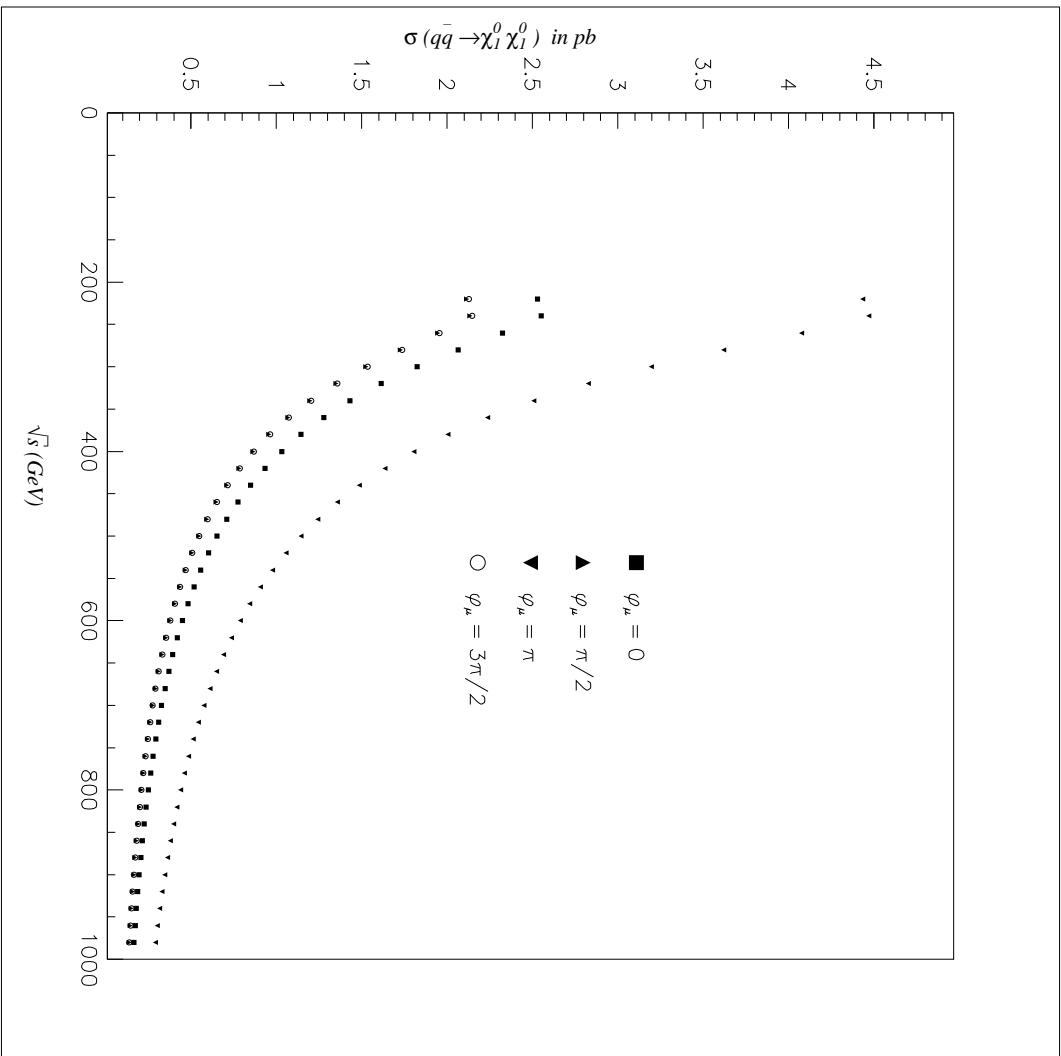


FIG. 10.

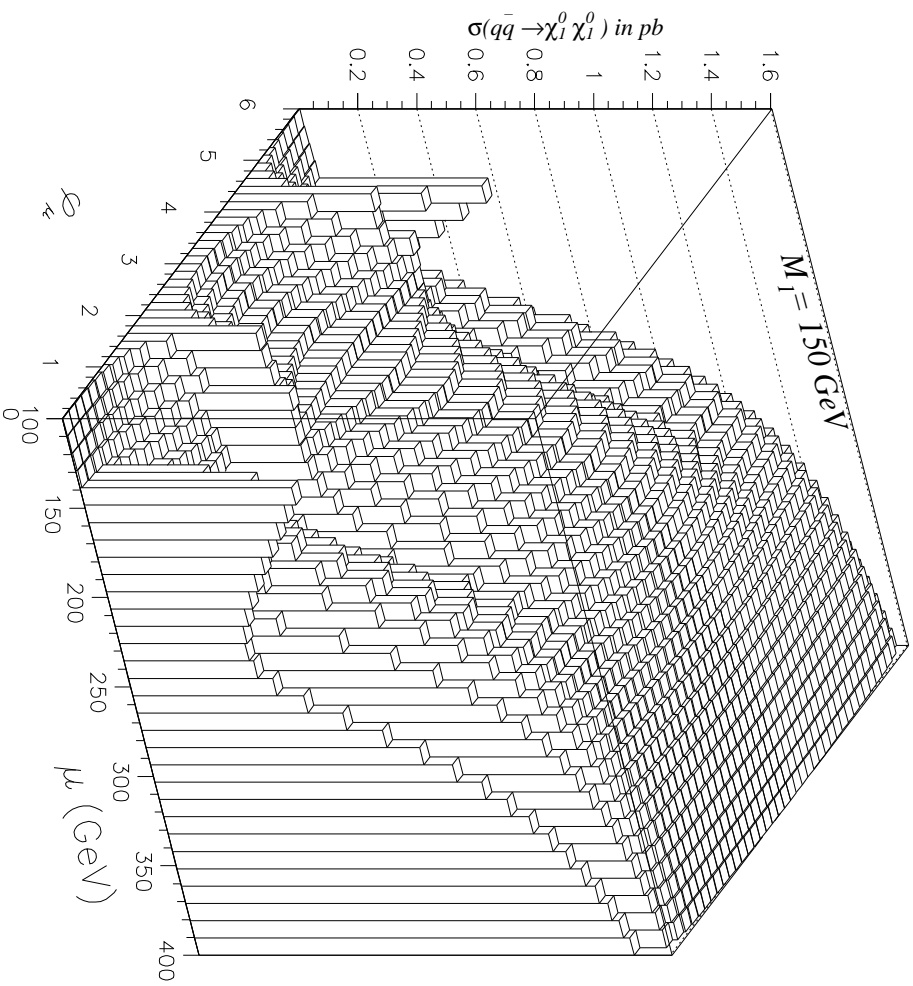


FIG. 11.

